Analytical Sciences (2022) 38:703–709
https://doi.org/10.1007/s44211-022-00088-5

ORIGINAL PAPER

The synthesis and characterization of iron nanoparticles with lemon peel and its use in magnetic solid phase extraction for trace levels of lead (II)

Emre Çakmak[1] · **Tülay Oymak**[1]

Received: 3 August 2021 / Accepted: 13 January 2022 / Published online: 3 March 2022

Abstract
In this study, a new magnetic solid phase extraction method (MSPE) was developed for the enrichment and separation of trace amount Pb(II) on the magnetic nanoparticles synthesized using lemon peel (Fe_3O_4-LP). The determination of Pb(II) in the samples was performed with inductively coupled plasma mass spectrometry. The Fe_3O_4-LP was characterized by scanning electron microscopy, X-ray powder diffractometry, Brunauer–Emmett–Teller surface area analysis, and vibration sample magnetometry. The effect of different parameters such as pH, adsorption and elution time, concentration of eluent and volume and matrix effect on the recovery of Pb(II) was investigated for the MSPE. Considering preconcentration factor, the detection limit value of the proposed method was calculated to be 39 ng/L for Pb (II). The accuracy of the developed method was tested with analysis of the BCR 185 R Bovine Liver and 2976a Mussel Tissue certified reference materials. The results were in good agreement with the certified values.

Keywords Lead (II) · Magnetic solid phase extraction · Inductively coupled plasma mass spectrometry · Lemon peel

Introduction

As trace elements and their species have an important effect on the ecological system and biological organisms, it is of great importance to determine the trace/ultra-trace levels of these in different samples to study biological effects and environmental pollution. Atomic spectrometry techniques such as flame atomic absorption spectrometry (FAAS), graphite furnace atomic absorption spectrometry (GFAAS), atomic fluorescence spectrometry (AFS), inductive coupled plasma-optical emission spectrometry (ICP-OES)] and inductive coupled plasma mass spectrometry (ICP-MS), are widely employed techniques in the analysis of trace elements and their species [1–7]. Of these atomic spectrometry techniques, ICP-MS has significant advantages due to low detection limit (LOD), wide dynamic linear range, multi-element/isotope analysis capability, and rapid detection. However, ICP-MS application for direct analysis of trace and ultra-trace elements in complex samples often suffers from the matrix effect [8–10]. Therefore, a sample preparation method is needed before determination by ICP-MS to separate the interfering sample matrix of the target element/species [11, 12]. Solid phase extraction (SPE) is one of the most widely used separation methods with ICP-MS determination, due to its simplicity, high recovery values, short extraction time, and low cost [13, 14]. The basic principle in solid phase extraction is to separate the target elements/species from the sample matrix and retain them on the adsorbent. The adsorbent is the most crucial factor affecting the selectivity/interference prevention ability, sensitivity, and extraction/desorption properties of the solid phase extraction method [13, 15]. Recently, the use of magnetic nanoparticles (MNPs) as adsorbents in SPE has attracted great interest as they have unique physical, chemical, and biological properties and a relatively large surface area compared to volume [16–18]. MNPs are nanoparticles that show magnetic properties, usually containing iron, nickel, cobalt elements and their oxides [19]. However, prepared MNPs are unstable and tend to agglomerate in the aqueous solution, and they have poor recyclability, low selectivity and capacity. To overcome this problem, different synthesis and surface modification strategies have been developed. Various chemicals, plants,

✉ Tülay Oymak
tulayoymak@cumhuriyet.edu.tr

[1] Faculty of Pharmacy, Department of Analytical Chemistry, Sivas Cumhuriyet University, Sivas 58140, Turkey

plant extracts, and plant waste have been used as coating reagent in the synthesis of MNPs [19–23]. In the last decade, the synthesis of MNPs with plants, plant extract and plant waste material has been of greater interest than chemical agents as they are low-cost, environmentally friendly, and the resulting products are both stable and controllable [24, 25]. Therefore, the use of various plants and plant parts (shell peel and leaf etc.) such as the leaf of *Camellia sinensis, Citrus paradisi,* the peel of *Punica granatum*, orange peel, *Pisum sativum*, coconut shell, and pomelo peel, have been investigated in the synthesis of MNPS by many researchers and have been the focus of attention [26–31]. The use of the solid phase extraction method (MSPE), in which magnetic nanoparticles are used as adsorbents as the separation method before ICP-MS analysis, has further improved the application potential of ICP-MS in complex sample analysis, minimizing sample/reagent consumption and pretreatment. This method has provided the opportunity to simplify the process.

In this study, magnetic nanoparticles were synthesized using the co-precipitation method with lemon peel and characterization was performed. The characterization of Fe_3O_4-LP used the methods of X-ray diffractometry (XRD), Scanning electron microscopy (SEM), Brunauer–Emmett–Teller (BET) surface area measurement and vibrating sample magnetometer (VSM). Then, a separation and enrichment method was developed and optimized using Fe_3O_4-LP as an adsorbent in the solid phase extraction of trace level Pb (II) ion before ICP-MS analysis. Finally, the accuracy of the method was verified with certified reference materials (BCR 185 R Bovine Liver ve 2976a Mussel Tissue).

Experimental

Materials

All the chemicals used were of analytical reagent grade. Hydrochloric acid (37%), sulphuric acid (98%), ammonia solution (26%) and ferrous sulfate pentahydrate were purchased from Sigma Aldrich (Steinheim, Germany). Suprapur Nitric acid 67–69% was obtained from Carlo Erba (Val de Reuil, France). Deionized water was used to prepare solutions of varying concentrations. The standard stock solution of 1000 mg/L Pb (II) and ferric chloride hexahydrate (99%), were purchased from Merck (Darmstadt, Germany). The standard stock solution of 1 mg/L was diluted from the original solution using deionized water with 2.0% nitric acid. Working standard solutions were prepared by successive dilution of the stock solution. Certified reference materials (CRMs) number 2976 were purchased from the National Standard Materials Center of US in Gaithersburg. The reference materials number 185 R Bovine Liver was obtained from the Community Bureau of Reference, Commission of the European Communities (Geel, Belgium). In magnetic separation for magnet made of neodymium with dimensions of 20*10*5 mm was used.

Instruments

An iCAP Q ICP-MS (Thermo Scientific, Germany) was used for Pb (II) analysis after the SPE procedure. The ICP-MS operating conditions are summarized in Table S1.The morphology of the initial lemon peel, Fe_3O_4 and Fe_3O_4-LP samples was analyzed on scanning electron microscope (TESCAN MIRA3 XMU Brno, Czechia). X-ray diffraction patterns were recorded with a Panalytical—Empyrean device (Almelo, Holland) using Cu Kα radiation ($\lambda = 0.15406$ nm, 40 mA, 45 kV). A continuous scan of 2 deg/min mode was used to collect 2θ data from 10 to 70 degrees, to determine the crystal structure of the samples. Magnetization studies were conducted (Lake Shore, 7407). M–H curves were measured with a maximum applied field of 20 kOe where parameters including saturation magnetization (Ms) were evaluated. Digestion of the samples was carried out in a microwave oven (CEM MARS 6, Matthews, USA) equipped with MarsXpress vessels for use in the acid digestion of the samples. The pH values were measured with a Mettler Toledo seven compact pH meter (Greifensee, Switzerland).

Samples digestions

Samples of tissue (0.025–0.1 g) and CRMs were weighed into a microwave vessel liner, and 5 mL of nitric acid (67–69%) was added. The liners were placed in vessels, closed with a sealed cap, and put into the microwave oven. The samples were digested applying the following microwave program parameters: ramp time: 20 min, hold time 15 min at 200 °C (cold 10 min). The extracts were diluted with deionized water to the final volume of 10 mL, then taken into another test tube and stored at 4 °C.

Synthesis of iron magnetic nanoparticles with lemon peel

The lemon peels were washed with deionized water and dried in an oven at 55 °C, then ground to powder in a mortar and sieved. The powdered lemon peels (LP) were used in the synthesis of iron magnetic nanoparticles using the co-precipitation method as previously reported [29, 32, 33]. To synthesize iron magnetic nanoparticles with lemon peel, first 6.1 g $FeCl_3.6H_2O$ was dissolved in 100 mL deionized water then, a few drops of concentrated HCl (37%) were added to prevent the precipitation of $Fe(OH)_3$, after which 4.2 g $FeSO_4.7H_2O$ was added and this solution was heated to

90 °C. A 1 g of lemon peel was dispersed in 100 mL deionized water for 1 h and 20 mL NH_3 (26%) was added rapidly to this solution at 90 °C. The mixture was stirred for 30 min at 90 °C, then cooled to room temperature. The resulting solid black material was collected with a strong magnetism permanent magnet, and washed several times with ethanol and deionized water. The resulting Fe_3O_4-LP was dried at 60 °C.

Fe_3O_4-LP based on magnetic solid phase extraction methods for Pb(II)

Model solutions containing 1 µg/L Pb (II) in 25 mL at pH 5 were prepared. The pH of the model solution was adjusted to the value pH 5 using 0.1 M CH_3COOH/0.1 M NH_3. Then, 50 mg Fe_3O_4-LP was added to the model solution to adsorb Pb (II) and the model solution was shaken for 1 min. A strong magnet was used to separate magnetic adsorbent from the liquid phase and the magnetic adsorbent was collected on the wall of the tube. The supernatant was discarded with a Pasteur pipette. Then, 2.5 mL of 3% HNO_3 was added to the test tube to elute the adsorbed Pb (II) on the surface on Fe_3O_4-LP and then, it was vortexed for 1 min. Again using a strong magnetism permanent magnet, Fe_3O_4-LP particles were collected on the wall of the tube. Eluent was withdrawn with a pipette into another test tube and the Pb (II) content in the eluent was determined with ICP-MS.

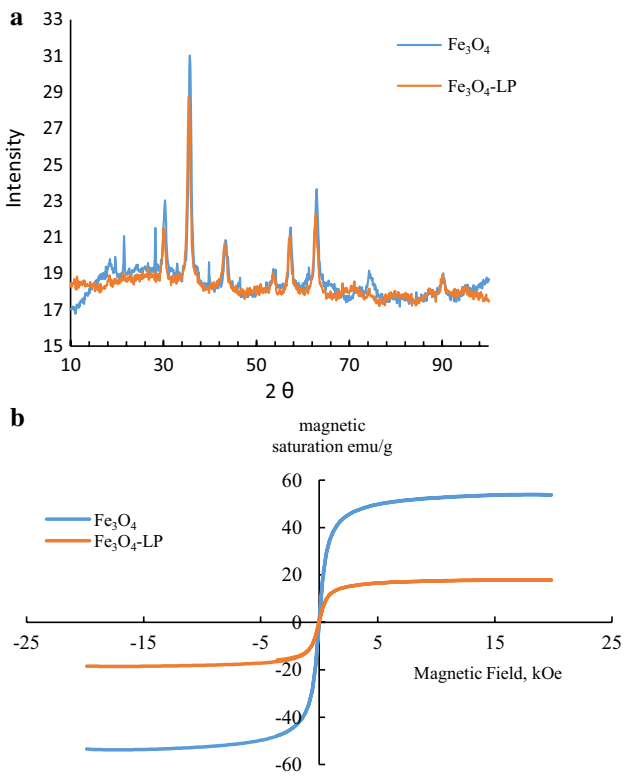

Fig. 2 **a** XRD patterns of Fe_3O_4 and Fe_3O_4-LP, **b** Magnetization curves of Fe_3O_4 and Fe_3O_4-LP

Result and discussion

The surface morphology of the lemon peels, Fe_3O_4 and the Fe_3O_4-LP nanoparticles was examined using SEM. The SEM images of the lemon peels, Fe_3O_4 and Fe_3O_4-LP nanoparticles are shown in Fig. 1. As can be seen in Fig. 1, after modification, the iron oxide particles were embedded in the LP matrices and structural changes occurred on the surface of Fe_3O_4 after the LP modification.

Fe_3O_4-LP and Fe_3O_4 were characterized by XRD (Fig. 2a). The peaks were obtained at 21.5 (111), 30.3 (220), 35.7 (311), 43.3 (400), 54.1 (422), 57.3 (511) and 62.9 (440). These peaks show that the major composition of MNP is Fe_3O_4 (magnetite) [34, 35]. The absence of a different diffraction peak in the XRD pattern of MNP indicates that there are no impurities in the product obtained. The decrease in the intensity of the peaks of Fe_3O_4-LP can be explained by the interaction between Fe_3O_4 and LP. The average nanoparticle diameter for Fe_3O_4 and Fe_3O_4-LP was calculated using the following Debye–Scherrer equation:

$$D_{\mathrm{HKL}} = \frac{k.\lambda}{B(2\theta).\cos\theta},$$

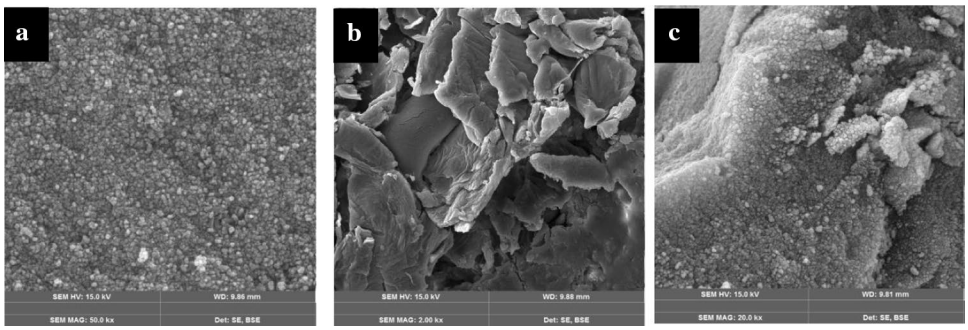

Fig. 1 SEM images of **a** Fe_3O_4, **b** LP, **c** Fe_3O_4-LP

where D is the mean nanoparticle diameter, λ; X-ray wavelength, B (2θ); half maximum width of the corresponding peak, and θ: the angle of the corresponding peak.

The average nanoparticle diameter of Fe_3O_4 and Fe_3O_4-LP was calculated as 12.1 nm and 11.7 nm using the peak with a 2θ value of 35.7°, which was the most intense peak.

In the magnetometry device to measure magnetic saturation, the hysteresis curves were measured. Magnetization curves were obtained by applying a 20 kOe magnetic field at 288 K. The magnetic saturation of Fe_3O_4 and Fe_3O_4-LP according to the data obtained from the vibrating magnetometry device was 53.8 emu/g and 18.2 emu/g, respectively. It can be seen from the magnetic curves (Fig. 2b) that superparamagnetic properties are exhibited. Magnetic adsorbents which have superparamagnetic properties have excellent advantages such as fast, convenient, and efficient magnetic separation in MSPE [36]. When an external magnetic field is applied to Fe_3O_4-LP, it can be easily and quickly separated from the aqueous medium.

The calculated BET surface area of Fe_3O_4-LP and Fe_3O_4 was 97.9 m^2/g, and 85.3 m^2/g, respectively. According to the analysis results, the surface area of Fe_3O_4-LP was larger than that of Fe_3O_4 and the average pore radius was smaller. The surface area properties of lemon peel, Fe_3O_4 and Fe_3O_4-LP are given in Table 1.

To determine the point of zero charge (pzc) for Fe_3O_4-LP, the pH of the solutions containing 0.1 mol/L $NaNO_3$ was adjusted to between 2 and 8 using 0.1 mol/L $HN0_3$ and 0.1 mol/L NaOH solutions [37]. Then, each solution was added to 50 mg of adsorbent and shaken at 25 °C for 24 h. The magnetic adsorbent and supernatant solutions were separated using a magnet and the pH of the supernatant solutions was measured with a pH meter. The changes of the pH (ΔpH) were plotted against the initial pH (pH_0) and pzc was calculated as 3.9 from the point where the curve crosses zero. The surface charge of Fe_3O_4-LP was determined to be negative when pH was > 3.9. Fe_3O_4-LP is expected to absorb cations at pH higher than 3.9 pH due to the negative charge of its surface (Fig. S1).

Table 1 Surface area and pore characteristics of lemon peel, Fe_3O_4, and Fe_3O_4-LP

Surface properties			
	BET surface area, m^2/g	Pore volume, cm^3/g	Average pore radius, °A
Lemon Peel	15.0	0.03	30.4
Fe_3O_4	85.3	0.29	57.8
Fe_3O_4-LP	97.9	0.22	39.9

Effect of pH

pH is an important parameter for recovery of trace elements in solid phase extraction. The pH of a solution affects balances such as the protonation/deprotonation of the adsorbed ion and the surface, and the groups attached to the surface. Therefore, first, the effect of the solution pH was examined in the separation and enrichment of Pb (II). Model solutions containing 1 µg/L Pb (II) were adjusted to the desired pH value by buffer solution. 50 mg of magnetic adsorbent (Fe_3O_4-LP) was added into model solutions and 5 min of shaking, by the rotator. The magnetic adsorbents were separated using an external magnet. Then, the supernatant was discarded by decantation. 5 mL of 5% HNO_3 solution as eluent was added onto the separated magnetic adsorbent and vortexed for 5 min. Afterward, the eluent and adsorbent were separated using a magnet again. Pb (II) concentrations in the eluent were determined by ICP-MS. The effect of pH on the recovery values of Pb (II) ions is shown in Fig. 3. The quantitative recovery value (≥ 95%) for Pb (II) ions was obtained at pH 4–8. Therefore, pH 5 was chosen as the optimum pH for subsequent experiments.

The effect of adsorption and elution time

The effect of adsorption and elution time on the separation and enrichment of Pb (II) ion with Fe_3O_4-LP was examined at pH 5 with 50 mg Fe_3O_4-LP in 25 mL. Adsorption interaction time and elution interaction time were studied for 1, 2, 4, 6 and 8 min.

The % recovery values of Pb (II) ion for each adsorption and elution interaction time were calculated as the average of three parallel run results. For Pb (II) ion at all examined adsorption and elution times, a recovery value of ≥ 95% was obtained. Both adsorption time and elution time of 1 min were used in the subsequent experiments (Fig. S2).

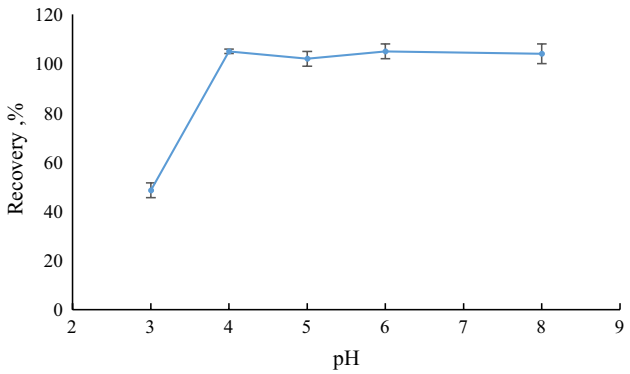

Fig. 3 Effect of pH on recovery of Pb(II) ions

Effect of eluent concentration and volume

The effect of the concentration and volume of the eluent on the quantitative recovery of the Pb (II) ion attached in the adsorbent was investigated. The MSPE method was applied with 25 mL model solutions containing 50 mg adsorbent and 1 µg/L Pb (II) ion at pH 5. To elute the adsorbed Pb (II) ions, 5 mL of 5% HNO_3, 5 mL of 3% HNO_3, 5 mL of 2% HNO_3 and 5 mL of 1% HNO_3 solutions were used. When 1%, 2%, 3% and 5% HNO_3 solutions were used as eluent the recovery value for Pb (II) ion was obtained as 84%, 95%, 96%, and 96%, respectively. The optimum eluent selected was 5 mL of 3% HNO_3. The results are shown in Fig. S3. After selecting the eluent concentration of 3% HNO_3, the effect of 2.5 mL eluent volume on the recovery of Pb (II) ion was investigated. Under optimum conditions, the recovery value of Pb (II) ion was 95% with 2.5 mL of 3% HNO_3 as the eluent. In the subsequent experiments, 2.5 mL of 3% HNO_3 was used as the eluent.

Effect of matrix ions

The developed MSPE method was applied to 25 mL model solutions containing different concentrations of Na (I), Mg (II), Ca (II), Cr (III), Al (III), Zn (II), Cd (II), Fe (III) Cu (II) and Ni (II) ions. As can be seen from Table 2, the described method separated Pb ions from matrix ions quite well and the concentration of matrix ions in the eluate solution was very low. The recovery % of other metal ions with concentrations ≥ 1000 higher than that of 1 µg/L Pb (II) are shown in Fig. 4. The results indicate that Fe_3O_4-LP has good selectivity for Pb(II).

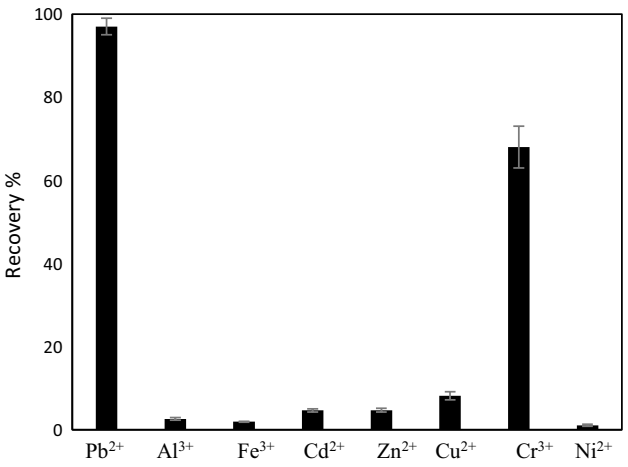

Fig. 4 Selectivity of the Fe_3O_4-LP for 1 µg/L Pb^{2+}, 5000 µg/L interference metal ions (concentration of Fe^{3+} is 1000 µg/L)

Capacity of Fe_3O_4-LP for Pb (II)

To examine the adsorption capacity of Fe_3O_4-LP, model solutions containing 200 mg/L Pb (II) in 25 mL at pH 5 were prepared. After adding 50 mg Fe_3O_4-LP to the model solution, the prepared solution was shaken for 1 h by a rotator. A strong magnet was used to separate the magnetic adsorbent from the supernatant. The supernatant was transferred by a pipette into another tube. The concentration of Pb (II) in the supernatant was determined by ICP-MS after 500 fold dilution with 5% HNO_3 solution. The same adsorption procedure was applied to without lemon peel prepared Fe_3O_4 magnetic nanoparticles. The adsorption capacity of Fe_3O_4 and Fe_3O_4-LP for Pb(II) was calculated using the following equation.

Table 2 Effect of matrix ions on recovery of Pb (II) 1 µg/L ($n = 3$)

Matrix ions	Added Salt	Concentration of matrix ion in model solution (mg/L)	Recovery % ± SD
Ca^{2+}	$Ca(NO_3)_2.4H_2O$	1000	102 ± 5
Na^{+}	NaCl	1000	108 ± 13
Mg^{2+}	$Mg(NO_3)_2.4H_2O$	1000	93 ± 6
Cd^{2+}	$Cd(NO_3)_2$	5	111 ± 1
Zn^{2+}	$Zn(NO_3)_2$	5	104 ± 7
Al^{3+}	$Al(NO_3)_3$	5	101 ± 6
Cr^{3+}	$Cr(NO_3)_2.9H_2O$	5	101 ± 7
Ni^{2+}	$Ni(NO_3)_2$	5	102 ± 3
Fe^{3+}	$Fe(NO_3)_3.9H_2O$	1	110 ± 2
NO_3^{-}	$Ca(NO_3)_2.4H_2O$	3000	102 ± 5
Cl^{-}	NaCl	1500	108 ± 13

$$q_e = \frac{v(C_0 - Ce)}{W},$$

where q_e, capacity of adsorbent (mg/g); V, volume (mL); C_0, initial concentration (µg/mL); Ce, equilibrium concentration (µg/mL) and W, amount of adsorbent (g).

The adsorption capacity of Fe_3O_4-LP and Fe_3O_4 magnetic nanoadsorbents for Pb (II) were 93.1 ± 1.3 mg/g and 48.2 ± 4.5 mg/g, respectively. The larger capacity of Fe_3O_4-LP magnetic nanoadsorbent can be explained by the fact that the surface area is larger than that of Fe_3O_4 and the average pore radius is small.

Analytical figures of merit

The precision and limit of detection (LOD) of the suggested method for Pb(II) determination were examined. When calculating the limit of detection, the optimized MSPE method was applied to ten 25 mL blank solutions. The limit of detection (LOD) and limit of quantification (LOQ) were calculated according to 3Sb/b and 10 Sb/b, respectively, where Sb is the standard deviation of blank signals and b is the slope of the calibration curve.

The LOD was found to be 39 ng/L and the LOQ was 129 ng/L with a preconcentration factor of 10. The preconcentration factor (PF) was calculated as the ratio of the highest sample volume and the lowest final volume. With 25 mL optimal sample volumes and final eluent volume of 2.5 mL, a preconcentration factor of 10 was calculated.

The interday and intra-day precision of the method (as relative standard deviation, RSD %) was determined by performing five cycles from a solution containing 1 µg/L Pb (II) and these values were found to be 5.5% and 3.4%, respectively.

The linear range of standard curve for Pb (II) without using the developed method were found to be 0.1–50 µg/L with the equation of $y = 0.0598x + 0.012$ ($R^2 = 0.9998$). The analytical parameters are summarized in Table 3.

Table 3 Analytical performance parameters of the method for Fe_3O_4-LP

Parameter	Value
Preconcentration factor	10
Capacity of Adsorption	93.1 mg/g
Limit of detection (with PCF)	39 ng/L
interday precision (RSD %)	5.5
intra-day precision (RSD %)	3.4
Linear Range	0.1–50 µg/L
Correlation coefficient (R^2)	0.9998

Analysis of lead in real samples

To test the accuracy of the developed method, certified reference materials were analyzed under optimum conditions. The developed MSPE method was applied to tissue samples and standard reference materials. Then, Pb (II) concentrations in the samples were measured by ICP-MS. The analysis results are given in Tables 4 and 5.

The developed method was applied to cattle liver, kidney, muscle, and lung samples taken from a local slaughterhouse in Sivas. These samples were prepared as explained in Sect. 2.3 before the method was applied. The results are given in Table 5.

Conclusion

In this study, a novel Fe_3O_4-LP was prepared and MSPE was applied for the determination of trace Pb followed by ICP-MS detection. The prepared Fe_3O_4-LP was seen to have good saturation magnetization values and high adsorption capacity for Pb(II). The benefits of the suggested method are simplicity of the operation, rapidity, good repeatability, low detection limit and low cost. The comparisons of different analytical techniques for the determination of Pb (II) are presented in Table S2. Compared with the other established methods, the method described here provided low LOD, good anti-interference ability, fast adsorption and elution time and is suitable for the determination of trace Pb (II) in real samples.

Table 4 The results of certified reference materials ($n = 3$)

	Certificated Value (µg/g)	Found Value (µg/g)
BCR 185 R Bovine Liver	0.172 ± 0.009	0.162 ± 0.020
2976a Mussel Tissue	1.19 ± 0.180	1.12 ± 0.130

Table 5 The results of real samples ($n = 3$)

Sample	Found Value (µg/g)
Liver	0.057 ± 0.001
Kidney	0.034 ± 0.002
Muscle	0.104 ± 0.007
Lungs	< LOQ

LOQ limit of quantitation

Supplementary Information The online version contains supplementary material available at https://doi.org/10.1007/s44211-022-00088-5.

Acknowledgements This research was supported by the Scientific Research Project Fund of Sivas Cumhuriyet University under the project number ECZ-064.

Declarations

Conflict of interests The authors have no conflict of interests to declare.

References

1. E. Koosha, M. Shamsipur, F. Salimi, M. Ramezani, Sep. Sci. Technol. **00**, 1 (2020)
2. N.J. Miller-Ihli, Anal. Chem. **64**(20), 964A-968A (1992)
3. F. Mohamed, D. Guillaume, N. Abdulwali, K. Al-Hadrami, M.A. Maher, Heliyon **6**, e04908 (2020)
4. A. Karasakal, Food. Anal. Methods **14**(2), 344–360 (2020)
5. R. Tedesco, M.C. Villoslada Hidalgo, M. Vardè, N.M. Kehrwald, C. Barbante, G. Cozzi, Food Control **121**, 107595 (2021)
6. W.T. Corns, P.B. Stockwell, L. Ebdon, S. J. Hill **8**, 71 (1993)
7. P. Chaikhan, Y. Udnan, R.J. Ampiah-Bonney, W.C. Chaiyasith, Anal. Sci. **37**, 1015 (2021)
8. J. Yin, Z. Jiang, G. Chang, B. Hu, Anal. Chim. Acta **540**, 333 (2005)
9. N. Zhang, H. Peng, S. Wang, B. Hu, Microchim. Acta **175**, 121 (2011)
10. S. Su, B. Chen, M. He, B. Hu, Z. Xiao, Talanta **119**, 458 (2014)
11. X. Jia, D. Gong, J. Zhao, H. Ren, J. Wang, X. Zhang, Microchim. Acta (2018). https://doi.org/10.1007/s00604-018-2766-x
12. H. Peng, N. Zhang, M. He, B. Chen, B. Hu, Talanta **131**, 266 (2015)
13. J. Qin, Z. Su, Y. Mao, C. Liu, B. Qi, G. Fang, S. Wang, Ecotoxicol. Environ. Saf. **208**, 111729 (2021)
14. H.N. Alharbi, A.O. Alsuhaimi, Glob. Nest J. **22**, 306 (2020)
15. S. Berijani, M.R. Ganjali, H. Sereshti, S.H. Tabatabaei, P. Norouzi, J. Iran. Chem. Soc. **12**, 737 (2015)
16. H.Z. Liu, J.J. Tang, X.X. Ma, L. Guo, J.W. Xie, Y.X. Wang, Anal. Sci. **27**, 19 (2011)
17. J. Xi, J. Zhang, H. Zhao, Anal. Sci. **33**, 999 (2017)
18. N. Pourreza, R. Zadeh-Dabbagh, Anal. Sci. **37**, 1213 (2021)
19. M. Wierucka, M. Biziuk, TrAC -. Trends Anal. Chem. **59**, 50 (2014)
20. G. Giakisikli, A.N. Anthemidis, Anal. Chim. Acta **789**, 1 (2013)
21. M. Hidarian, S. Hashemian, Orient. J. Chem. **30**, 1753 (2014)
22. B. Maddah, J. Shamsi, J. Chromatogr. A **1256**, 40 (2012)
23. X. Qin, A.A.A. Bakheet, X. Zhu, J. Iran. Chem. Soc. **2017**, 14 (2017)
24. P. Karpagavinayagam, C. Vedhi, Vacuum **160**, 286 (2019)
25. S. Saif, A. Tahir, Y. Chen, Nanomaterials **6**, 1 (2016)
26. B. Kumar, K. Smita, S. Galeas, V. Sharma, V.H. Guerrero, A. Debut, L. Cumbal, Inorg. Chem. Commun. **119**, 108116 (2020)
27. S. Venkateswarlu, B.N. Kumar, B. Prathima, Y. SubbaRao, N.V.V. Jyothi, Arab. J. Chem. **12**, 588 (2019)
28. C. Prasad, G. Yuvaraja, P. Venkateswarlu, J. Magn. Magn. Mater. **424**, 376 (2017)
29. V.K. Gupta, A. Nayak, Chem. Eng. J. **180**, 81 (2012)
30. Z. Hao, C. Wang, Z. Yan, H. Jiang, H. Xu, Chemosphere **211**, 962 (2018)
31. V.H. Nguyen, H.T. Van, V.Q. Nguyen, X. Van Dam, L.P. Hoang, L.T. Ha, L.T. Ha, J. Chem. (2020). https://doi.org/10.1155/2020/3080612
32. J. Yang, Q. Zeng, L. Peng, M. Lei, H. Song, B. Tie, J. Gu, J. Environ. Sci. (China) **25**, 413 (2013)
33. C. He, J. Qu, Z. Yu, D. Chen, T. Su, L. He, Z. Zhao, C. Zhou, P. Hong, Y. Li, S. Sun, C. Li, Nanomaterials **9**(7), 953 (2019)
34. H. El Ghandoor, H.M. Zidan, M.M.H. Khalil, M.I.M. Ismail, Int. J. Electrochem. Sci. **7**, 5734 (2012)
35. W.S. Peternele, V. Monge Fuentes, M.L. Fascineli, J. Rodrigues Da Silva, R.C. Silva, C.M. Lucci, R. Bentes De Azevedo, J. Nanomater. (2014). https://doi.org/10.1155/2014/682985
36. S. Ali, S. A. Khan, Z. H. Yamani, M. T. Qamar, M. A. Morsy, and S. Sarfraz, Shape- and size-controlled superparamagnetic iron oxide nanoparticles using various reducing agents and their relaxometric properties by Xigo acorn area, **2019**.
37. S. Bakhshi Nejad, A. Mohammadi, J. Chem. Eng. Data **65**, 2731 (2020)